Color evaporation description of inelastic photoproduction of J/ψ at DESY HERA

O. J. P. Éboli*
Instituto de Física, Universidade de São Paulo, São Paulo, SP, Brazil

E. M. Gregores†
Instituto de Física Teórica, Universidade Estadual Paulista, São Paulo, SP, Brazil

F. Halzen‡
Department of Physics, University of Wisconsin, Madison, Wisconsin 53706

(Received 8 November 2002; published 10 March 2003)

The H1 Collaboration recently reported a new analysis of data on the inelastic photoproduction of J/ψ mesons at DESY's HERA *ep* collider. We show that these new experimental results are well described by the color evaporation model for quarkonium production. Moreover, these new data require the introduction of resolved photon contributions in order to accommodate the results in the kinematic region where the fractional energy carried by the J/ψ is small, demonstrating that colored perturbative $c\bar{c}$ states contribute to the production of a color singlet.

DOI: 10.1103/PhysRevD.67.054002 PACS number(s): 13.60.Le, 25.20.Lj

I. INTRODUCTION

The H1 Collaboration recently reported new data on the inelastic photoproduction of J/ψ mesons [1] as well as a comparison with the color singlet [2] and color octet [3] models. We here compare the H1 data with the color evaporation model (CEM) for quarkonium production showing that it also provides a good description of the same data. These data probe for the first time the production of charmonium states carrying a small energy fraction (z), requiring the introduction of resolved photon contributions in order to explain the results. These contributions are color octet configurations, clearly confirming the necessity to include them in the charmonium production mechanism.

In contrast with a wealth of information on charmonium production elsewhere, previous measurements of the inelastic photoproduction of charmonium at the DESY *ep* collider HERA [4,5] appeared to indicate that color octet models failed to describe the data for a large charmonium energy fraction z. In contrast, the color singlet model fits the large z data well. To solve this puzzle, we argued [6] that this discrepancy resulted from the neglect of non-perturbative effects that are important at large z. Implementing a phenomenological parameterization of these effects in a scheme originally developed for Drell-Yan phenomenology, we illustrated that agreement with data could be achieved. In this work, we employ the same procedure of [6] to parametrize the non-perturbative effects important at large z.

II. THEORETICAL FRAMEWORK

The failure of the color singlet model [7] to describe the charmonium production at the Fermilab Tevatron [8] is in sharp contrast with a simple and successful picture that J/ψ production is a two-step process where a heavy quark pair is produced first in any color state, followed by the nonperturbative formation of the colorless asymptotic state. In other words, color octet as well as singlet $c\bar{c}$ states contribute to the production of J/ψ. Several formalisms have been proposed to incorporate these basic features: the nonrelativistic QCD (NRQCD) method [9], the CEM scheme [10,11], and the soft color interaction model [12]. The original CEM [13] actually predates the color singlet approach, and had been abandoned for no good reason. Recent measurements of the polarization of bound charm and beauty mesons are clearly at variance with the NRQCD framework [14]; one may argue however that we need more data and more precise calculations to come to a firm conclusion.

The formation of charmonium states has two different scales: the scale of the hard subprocess describing the creation of the $c\bar{c}$ pair is m_ψ^{-1}, while the hadronization scale is Λ_{QCD}. Therefore, $c\bar{c}$ pairs formed at short distances live long enough for soft gluons to readjust the color of the pairs before they appear as asymptotic ψ, χ_c or, alternatively, $D\bar{D}$ states. The CEM simply states that charmonium production is described by the same dynamics as $D\bar{D}$ production, i.e., by the formation of a colored $c\bar{c}$ pair. The formation of color-singlet states, rather than colored pairs, is the result of a non-perturbative process involving large-distance color fluctuations, and is modeled by a statistical counting of possible color final states. This same approach to color provides a successful description of the production of rapidity gaps between jets at the Tevatron [15–19] and HERA [17,18] as well as the formation of forward rapidity gaps at HERA [20,21].

The CEM predicts that the sum of the cross section of all onium and open charm states is described by [10,19]

$$\sigma_{\text{onium}} = \frac{1}{9}\int_{2m_c}^{2m_D} dM_{c\bar{c}} \frac{d\sigma_{c\bar{c}}}{dM_{c\bar{c}}}, \tag{1}$$

*Electronic address: eboli@fma.if.usp.br
†Electronic address: gregores@ift.unesp.br
‡Electronic address: halzen@pheno.physics.wisc.edu

 ©2003 The American Physical Society

and

$$\sigma_{\rm open}=\frac{8}{9}\int_{2m_c}^{2m_D} dM_{c\bar{c}}\,\frac{d\sigma_{c\bar{c}}}{dM_{c\bar{c}}}+\int_{2m_D} dM_{c\bar{c}}\,\frac{d\sigma_{c\bar{c}}}{dM_{c\bar{c}}}, \quad (2)$$

where $M_{c\bar{c}}$ is the invariant mass of the $c\bar{c}$ pair. The factor 1/9 stands for the probability that a pair of charm quarks formed at a typical time scale $1/M_\psi$ ends up as a color singlet state after exchanging soft gluons with the final state remnants. This factor reflects the fact that there is one color singlet state out of 9 possible color configurations of a $c\bar{c}$ pair. One attractive feature of this model is the intimate relation between the production of charmonium and of open charm which allows us to use open charm data to perform the perturbative QCD calculation, and to subsequently make direct predictions for charmonium cross sections.

The fraction ρ_ψ of produced onium states that materialize as ψ,

$$\sigma_\psi=\rho_\psi\,\sigma_{\rm onium}, \quad (3)$$

has been inferred from low energy measurements to be a constant [22,23]. It is interesting to notice that the CEM has fewer free parameters than the other models, e.g., NRQCD; nevertheless, it successfully accommodates all features of charmonium production [3,24,25].

From the charmonium photoproduction, we determined that $\rho_\psi=0.43-0.5$ [11], a value that can be accounted for by statistical counting of final states [12]. The fact that all ψ production data are described in terms of this single parameter, fixed by J/ψ photoproduction, leads to parameter-free predictions for the Z-boson decay rate into prompt ψ [26], and to charmonium production cross sections at Tevatron [27] and HERA [6], as well as for neutrino-initiated reactions [28]. These predictions are in agreement with the available data.

III. INELASTIC PHOTOPRODUCTION OF CHARMONIUM

The cross section for the J/ψ photoproduction at a given center-of-mass energy W is

$$\sigma_{\gamma p\to J/\psi X}(W)=\int\int f_{A/\gamma}(x_A)f_{B/p}(x_B)\hat{\sigma}_{AB\to J/\psi X}(\hat{s})dx_A dx_B, \quad (4)$$

where the subprocess CEM cross section $\hat{\sigma}$ is given by Eqs. (1) and (3). Here, $\sqrt{\hat{s}}=\sqrt{x_A x_B}\,W$ is the center-of-mass energy of the subprocess $AB\to J/\psi X$, and $f_{A/\gamma}$ ($f_{B/p}$) is the distribution function of the parton A (B) in the photon (proton). For direct photon interactions ($A=\gamma$) we have $f_{A/\gamma}(x_A)=\delta(x_A-1)$.

An important kinematical variable is

$$z\equiv\frac{P_{J/\psi}\cdot P_p}{P_\gamma\cdot P_p}, \quad (5)$$

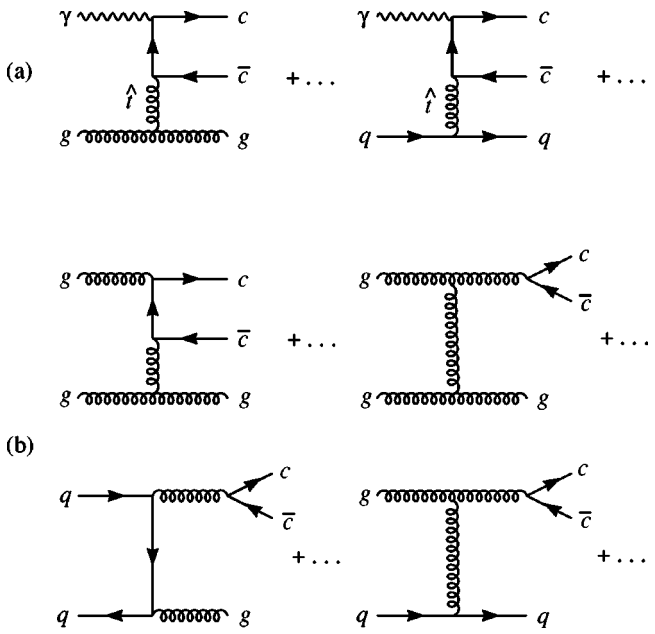

FIG. 1. Processes contributing to direct (a) and resolved (b) charmonium photoproduction.

where $P_{J/\psi,\gamma,p}$ is the four-momentum of the J/ψ, photon, or proton, respectively. In the proton rest frame, z is the fraction of photon energy carried by the J/ψ.

The direct photon process $\gamma g\to c\bar{c}$ is important only for $z\approx 1$. For the range of z we are interested in, the direct photon contribution is dominated by the diagrams shown in Fig. 1(a). The charm quark pair in γg fusion can be produced in both color singlet and octet configurations, while γq fusion exclusively yields colored $c\bar{c}$ pairs. J/ψ production also receives contributions from resolved photon processes, which proceed via quark-quark, quark-gluon, and gluon-gluon fusion into $c\bar{c}+$quark (gluon); see Fig. 1(b).

Higher order processes, like those in Fig. 1, have to be evaluated with some caution in the region of small J/ψ transverse momentum and large z. For small t-channel momentum transfer ($\hat{t}\to 0$), the gluon exchange diagrams in Fig. 1 represent the QCD evolution of the initial state gluon distribution functions, and are already included in the lowest order $\gamma g\to c\bar{c}$ process [29]. By themselves, the tree level diagrams in Fig. 1 lead to a divergence for $z\to 1$, which appears as an unphysical growth of the cross section for $z\lesssim 1$.

Presently, complete QCD calculations are not available for the processes we are interested in. Therefore, nonperturbative effects and higher order QCD corrections at large z are treated by phenomenological methods. We describe charmonium photoproduction by introducing the following parametrization:

$$\frac{d^2\sigma}{dp_T dz}=[1-F(Q_0,p_T)][1-G(Q_0,z)]\frac{d^2\sigma_{\rm tree}}{dp_T dz} \quad (6)$$

with

$$F(Q_0,p_T)=e^{-p_T^2/k_T^2} \quad (7)$$

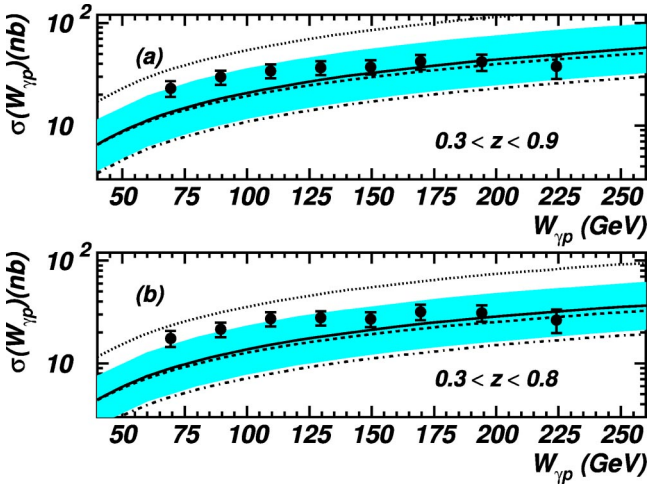

FIG. 2. Total cross section as a function of $W_{\gamma p}$ for $p_T > 1$ GeV: (a) $0.3<z<0.9$ and (b) $0.3<z<0.8$. The shaded band shows the theoretical prediction for $m_c = 1.3 \pm 0.1$ GeV. The definition of the lines is given in the text.

and

$$G(Q_0,z) = e^{-(1-z)/z_0 z}; \tag{8}$$

see Ref. [6] for further details. Here, $\sigma_{\rm tree}$ is the tree level perturbative cross section, $k_T^2 = z(Q_0^2 + 4m_c^2) - 4m_c^2$, and $(1-z_0) = (p_T^2 + 4m_c^2)/(Q_0^2 + 4m_c^2)$ are positive definite or null. We found in Ref. [6] that $Q_0 = 2m_c$ best describes the data, and it is this value that we use in the present work.

IV. RESULTS

We have computed the tree level scattering amplitudes numerically using MADGRAPH [30] and HELAS [31]. The phase space integration was performed using the VEGAS Monte Carlo program [32].

The H1 Collaboration performed their analysis using data with $Q^2 < 1$ GeV^2. They subdivided their data into several different kinematical regions, in order to better determine the region where perturbative QCD calculations furnish a reliable description of the data. We will compare the CEM predictions with the H1 results using the same cuts that were applied to the experimental data. First, we analyze the behavior of the total cross section as a function of the γp center-of-mass energy (W) for two different z regions, requiring a minimum J/ψ transverse momentum $p_T > 1$ GeV. In Fig. 2(a) we show the CEM predictions for $0.3<z<0.9$, and in Fig. 2(b) we present our results for $0.3<z<0.8$.

A relatively wide choice of QCD parameters associated with the evaluation of charmonium photoproduction leads to a large theoretical uncertainty. In Fig. 2, the solid lines are obtained assuming $m_c = 1.3$ GeV, the GRV-94 leading order (LO) [33] parametrization of the proton structure functions and GRV-G LO [34] for the photon parton density. For both structure functions, we set the factorization scale as $\mu_F = \sqrt{\hat{s}}$ and we evaluated the running of the strong coupling constant in leading order with four active flavors using $\Lambda_{\rm QCD} = 300$ MeV, renormalization scale $\mu_R^0 = \sqrt{2} m_c$ for direct processes, and $\mu_R^0 = \sqrt{\hat{s}}$ for resolved processes. We also use $\rho_\psi = 0.5$ as the J/ψ fraction of all charm bound states. The shaded band is obtained by varying the charm quark mass in the range $m_c = 1.3 \pm 0.1$ GeV.

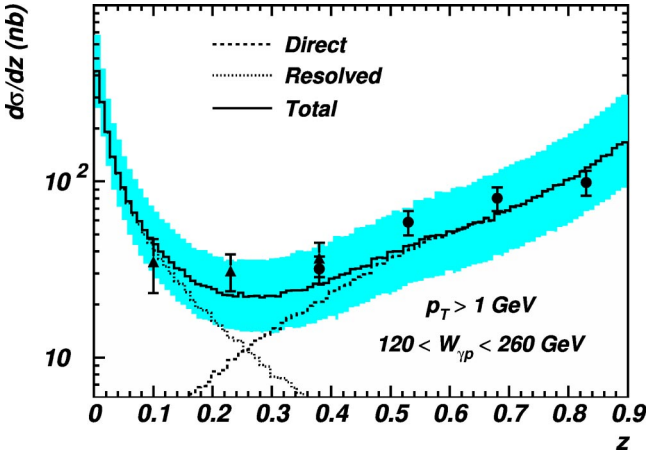

FIG. 3. Differential cross section as function of the inelasticity parameter z for $p_T^2 > 1$ GeV^2 and $120 < W_{\gamma p} < 260$ GeV. The dashed line stands for the contribution from direct processes while the dotted line shows the contribution from resolved processes. The solid line is the sum of both contributions. The shaded band shows the theoretical uncertainty associated with the charm quark mass ($m_c = 1.3 \pm 0.1$ GeV).

In order to assess the uncertainty associated with the proton structure function, we evaluate the CEM prediction using the same parameters as for the solid line, changing GRV-94 LO for GRV-98 LO [35]; the result is plotted as a dashed line. The dependence upon the structure function is quite mild. We estimate the effect of higher order corrections by varying the renormalization scale $\mu_R = \xi \mu_R^0$ while keeping the other parameters fixed. The dotted (dash-dotted) lines in Fig. 2 correspond to the choices $\xi = 1/2$ (2). For the sake of definiteness, we present subsequent results using the parameters associated with the solid line in Fig. 2 only varying the charm quark mass from $m_c = 1.3 \pm 0.1$ GeV.

Figure 3 shows the CEM predictions for the z spectrum, with $p_T > 1$ GeV and the center-of-mass energy in the range $120 < W_{\gamma p} < 260$ GeV. The experimental points represented by triangles and squares correspond to two different data sets; see Ref. [1] for details. The direct photon contribution is represented by the dashed line, and the resolved one by the dotted line; the solid line displays the sum of direct and resolved contributions. The shaded area corresponds to the total CEM prediction for the charm quark mass range described above. The agreement with the data is quite good. Moreover, the data at low and medium z do require the introduction of resolved processes in order to explain the results. This is a clear signal that colored charm quark pairs contribute to the J/ψ production.

In Fig. 4 we present the p_T^2 distribution for the low z sample $0.05<z<0.45$ which corresponds to the triangles in Fig. 3. For these values of z we expect the theoretical uncertainties due to higher order corrections to be small, and we can see that the CEM and data agree well. The disagreement

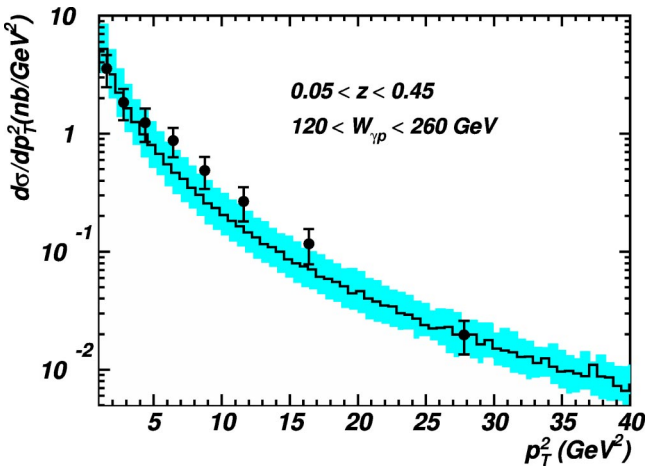

FIG. 4. Squared transverse momentum p_T^2 distribution for data collected in the very inelastic region $0.05<z<0.45$ and $120<W_{\gamma p}<260$ GeV. The shaded band shows the theoretical uncertainty associated with the value of the charm quark mass ($m_c=1.3\pm0.1$ GeV).

between data and theory at large z is associated with higher order non-perturbative corrections.

Higher order effects are sizeable in the medium and high z regions. Therefore, the H1 Collaboration divided their data sample into several p_T and z regions for center-of-mass energies in the range $60<W_{\gamma p}<240$ GeV. This allows us to make a better comparison of data and theory.

In Fig. 5, we compare the CEM predictions for the z dependence with data for three different values of the J/ψ minimum transverse momentum, i.e., $p_T>1,2$, and 3 GeV. The curves have been divided by factors 1,10, and 100, respectively, in order to help visualization. There is an overall agreement between data and theory, except for the highest bin in z. Moreover, removing our regularization procedure worsens the theoretical results [6]. Increasing the minimum

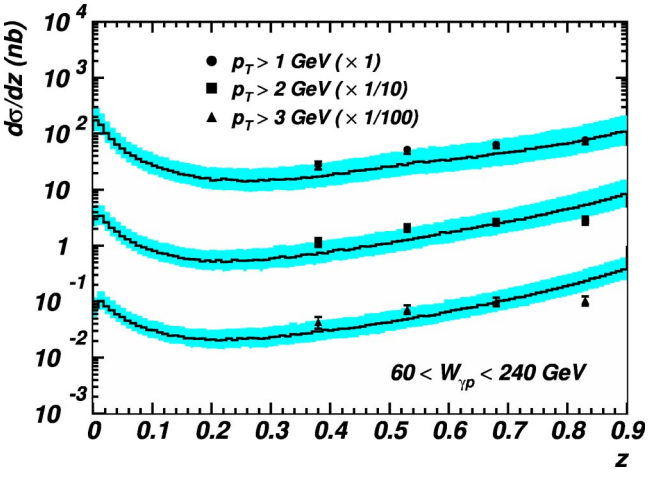

FIG. 5. Differential cross section as function of the inelasticity parameter z for $p_T>1,2$, and 3 GeV, divided by the factor 1, 10, and 100 respectively. The shaded band shows the theoretical uncertainty associated with the value of the charm quark mass ($m_c=1.3\pm0.1$ GeV).

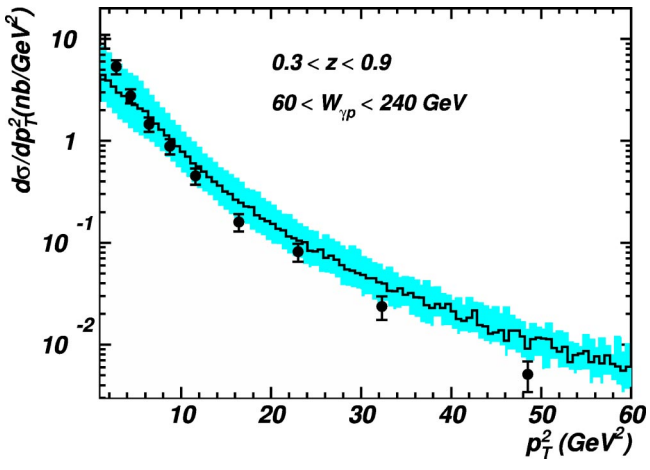

FIG. 6. Squared transverse momentum p_T^2 distribution for $0.3<z<0.9$ and center-of-mass energy $60<W_{\gamma p}<240$ GeV. The shaded band shows the theoretical uncertainty associated with the value of the charm quark mass ($m_c=1.3\pm0.1$ GeV).

value of the transverse momentum does not improve the quality of the fitting, indicating that our parametrization of the higher order effects correctly incorporates the dependence on the minimum p_T.

Figure 6 shows the J/ψ squared transverse momentum distribution for the medium and high-z data. The agreement between theory and data is satisfactory. The shape of the spectrum disagrees with data for the very low p_T bins. In order to understand what is happening, let us consider this distribution for three different z bins, $0.75<z<0.9$, $0.6<z<0.75$, and $0.3<z<0.6$; see Fig. 7. The predictions have been divided by factors 1,10, and 100, respectively, to help visualization. We learn from this figure that the agreement between CEM predictions and data improves for low z regions. This reflects a limitation of the ability of the proposed

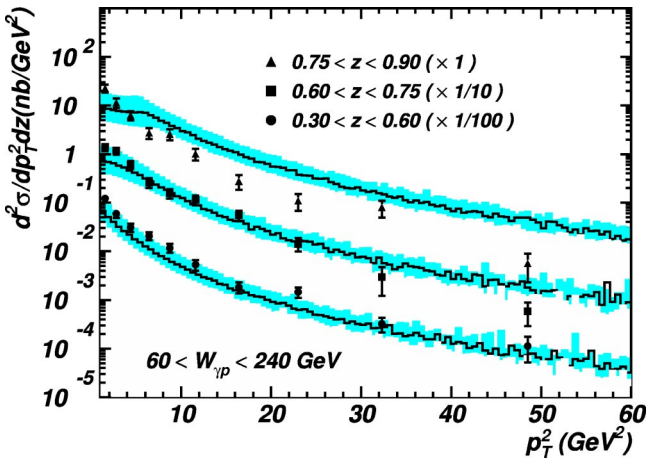

FIG. 7. Squared transverse momentum p_T^2 spectrum for $60<W_{\gamma p}<240$ and data collected in three different inelastic bins: $0.75<z<0.9$ (upper), $0.6<z<0.75$ (middle), and $0.3<z<0.6$ (lower). For visualization the curves have been scaled as 1, 1/10, and 1/100 from top to bottom. The shaded band shows the theoretical uncertainty associated with the value of the charm quark mass ($m_c=1.3\pm0.1$ GeV).

parametrization to completely mimic higher order QCD contributions when we approach the elastic region. It also implies that the small discrepancy with data for the highest bin on z must be credited to the lack of a complete QCD calculation and is not related to the color evaporation approach to describing quarkonium production.

V. CONCLUSIONS

We showed that the color evaporation model describes the available data on J/ψ photoproduction, provided that we include high order QCD corrections at high inelasticities z. Moreover, the new data at low z provide a clear demonstration of the necessity to consider colored $c\bar{c}$ configurations in the computation of charmonium production, since the data in this region can only be explained by resolved photon processes, which generate colored $c\bar{c}$ pairs.

ACKNOWLEDGMENTS

This research was supported in part by the University of Wisconsin Research Committee with funds granted by the Wisconsin Alumni Research Foundation, by the U.S. Department of Energy under grant DE-FG02-95ER40896, by Fundação de Amparo à Pesquisa do Estado de São Paulo (FAPESP), by Conselho Nacional de Desenvolvimento Científico e Tecnológico (CNPq), and by Programa de Apoio a Núcleos de Excelência (PRONEX).

[1] H1 Collaboration, C. Adloff *et al.*, Eur. Phys. J. C **25**, 25 (2002).
[2] M. Kramer, Nucl. Phys. **B459**, 3 (1996).
[3] M. Kramer, Prog. Part. Nucl. Phys. **47**, 141 (2001).
[4] H1 Collaboration, S. Aid *et al.*, Nucl. Phys. **B472**, 3 (1996).
[5] ZEUS Collaboration, J. Breitweg *et al.*, Z. Phys. C **76**, 599 (1997).
[6] O.J. Eboli, E.M. Gregores, and F. Halzen, Phys. Lett. B **451**, 241 (1999).
[7] R. Baier and R. Ruckl, Z. Phys. C **19**, 251 (1983).
[8] CDF Collaboration, F. Abe *et al.*, Phys. Rev. Lett. **69**, 3704 (1992); **79**, 572 (1997); **79**, 578 (1997); DØ Collaboration, S. Abachi *et al.*, Phys. Lett. B **370**, 239 (1996).
[9] G.T. Bodwin, E. Braaten, and G.P. Lepage, Phys. Rev. D **51**, 1125 (1995); **55**, 5853(E) (1997).
[10] J.F. Amundson, O.J. Eboli, E.M. Gregores, and F. Halzen, Phys. Lett. B **372**, 127 (1996).
[11] J.F. Amundson, O.J. Eboli, E.M. Gregores, and F. Halzen, Phys. Lett. B **390**, 323 (1997).
[12] A. Edin, G. Ingelman, and J. Rathsman, Phys. Rev. D **56**, 7317 (1997).
[13] H. Fritzsch, Phys. Lett. **67B**, 217 (1977); F. Halzen, *ibid.* **69B**, 105 (1977); F. Halzen and S. Matsuda, Phys. Rev. D **17**, 1344 (1978).
[14] CDF Collaboration, T. Affolder *et al.*, Phys. Rev. Lett. **85**, 2886 (2000).
[15] O.J. Eboli, E.M. Gregores, and F. Halzen, Nucl. Phys. B (Proc. Suppl.) **71**, 349 (1999).
[16] O.J. Eboli, E.M. Gregores, and F. Halzen, Phys. Rev. D **58**, 114005 (1998).
[17] O.J. Eboli, E.M. Gregores, and F. Halzen, Phys. Rev. D **61**, 034003 (2000).
[18] O.J. Eboli, E.M. Gregores, and F. Halzen, Nucl. Phys. B (Proc. Suppl.) **99A**, 257 (2001).
[19] O.J. Eboli, E.M. Gregores, and F. Halzen, in *Proceedings of the 26th International Symposium on Multiparticle Dynamics (ISMD 96)*, Faro, Portugal, 1996, edited by A. Mourão, M. Pimenta, R. Potting, and P. Sonderegger (World Scientific, Singapore, 1998), p. 35.
[20] W. Buchmüller, Phys. Lett. B **353**, 335 (1995); W. Buchmüller and A. Hebecker, *ibid.* **355**, 573 (1995).
[21] A. Edin, G. Ingelman, and J. Rathsman, Phys. Lett. B **366**, 371 (1996).
[22] R. Gavai *et al.*, Int. J. Mod. Phys. A **10**, 3043 (1995).
[23] G. Schuler, Report No. CERN-TH.7170/94.
[24] C.B. Mariotto, M.B. Gay Ducati, and G. Ingelman, Eur. Phys. J. C **23**, 527 (2002).
[25] G.A. Schuler and R. Vogt, Phys. Lett. B **387**, 181 (1996).
[26] O.J. Eboli, E.M. Gregores, and F. Halzen, Phys. Lett. B **395**, 113 (1997).
[27] O.J. Eboli, E.M. Gregores, and F. Halzen, Phys. Rev. D **60**, 117501 (1999).
[28] O.J. Eboli, E.M. Gregores, and F. Halzen, Phys. Rev. D **64**, 093015 (2001).
[29] P. Nason, S. Dawson, and R.K. Ellis, Nucl. Phys. **B303**, 607 (1988).
[30] W. Long and T. Steltzer, Comput. Phys. Commun. **81**, 357 (1994).
[31] H. Murayama, I. Watanabe, and K. Hagiwara, KEK Report No. 91-11.
[32] G.P. Lepage, Report No. CLNS-80/447.
[33] M. Gluck, E. Reya, and A. Vogt, Z. Phys. C **67**, 433 (1995).
[34] M. Gluck, E. Reya, and M. Stratmann, Phys. Rev. D **51**, 3220 (1995).
[35] M. Gluck, E. Reya, and A. Vogt, Eur. Phys. J. C **5**, 461 (1998).